Available online at www.sciencedirect.com
ScienceDirect
Journal of Molecular Catalysis A: Chemical 278 (2007) 145–151
JOURNAL OF MOLECULAR CATALYSIS A: CHEMICAL
www.elsevier.com/locate/molcata

Natural and H_2-reduced limonite for organic oxidation by a Fenton-like system: Mechanism study via ESI-MS and theoretical calculations

Wladmir F. de Souza [a,1], Iara R. Guimarães [b,2], Luiz C.A. Oliveira [b,*], Mário C. Guerreiro [b,2], Aline L.N. Guarieiro [b,2], Kele T.G. Carvalho [b,2]

[a] *CENPES-Petrobras, Cidade Universitária Q.7 Ilha do Fundão, CEP 21949-900, Rio de Janeiro, RJ, Brazil*
[b] *Universidade Federal de Lavras, Depto. Química, Caixa Postal, CEP 37200-000, Lavras, MG, Brazil*

Received 5 July 2007; received in revised form 27 August 2007; accepted 1 September 2007
Available online 7 September 2007

Abstract

A Fenton-like system based on iron oxide surface modification by thermal treatment under H_2 flow was investigated. The materials were characterized by powder X-ray diffraction (XRD), chemical analyses, scanning electron microscopy (SEM), temperature programmed reduction (TPR) and ^{57}Fe Mössbauer spectroscopy. Results showed that the main iron oxides phases in the thermal treated material were goethite (α-FeOOH) and magnetite (Fe_3O_4). A decomposition study was carried out using a basic dye as a model compound (methylene blue). The reactions were monitored by electrospray ionization mass spectrometry (ESI-MS), revealing that the methylene blue dye was successively oxidized (hydroxylations) forming different intermediaries species. These results strongly suggest that highly reactive hydroxyl radicals generated from the reaction of H_2O_2 on the catalysts surface were responsible for the dye oxidation, proving that the material act as an efficient heterogeneous Fenton-like catalyst. Theoretical quantum mechanics calculations, DFT, were carried out in order to understand the degradation mechanism for methylene blue with goethite.

Keywords: Goethite; Fenton-like; Organic oxidation; ESI-MS; Mössbauer spectroscopy

1. Introduction

Limonite is a natural ore comprised of hydrated iron(III) oxides, mostly made up of goethite (α-FeOOH). Recently, a Fenton-like system that combines H_2O_2 with an organic acid (*e.g.* HCOOH) and an iron oxide (natural limonite ore) was developed [1]. This combined aqueous slurry system is able to perform oil phase oxidation and simultaneous removal of instable hydrocarbons and heteroatom compounds from hydrocarbon streams, such as petroleum distillates [2,3]. However, the mechanism of Fenton oxidant formation was not fully understood.

The Fenton reaction ($Fe^{2+} + H_2O_2 \rightarrow Fe^{3+} + {}^{-}OH + {}^{\bullet}OH$), involving hydrogen peroxide and Fe^{2+} in solution, is used to degrade contaminants, such as textile dyes, present in industrial wastewaters [4]. In order to minimize the amount of the forming ferric hydroxide sludge in this homogeneous reaction [5], some iron oxides such as magnetite (ideal formula, Fe_3O_4), hematite (α-Fe_2O_3), goethite (α-FeOOH) or ferrihydrite ($Fe_5HO_8{\cdot}4H_2O$) have been used instead of Fe^{2+} solutions [6,7]. The active heterogeneous redox processes are increasingly replacing the homogeneous systems in the catalysis research [8,9] and in some technological applications, such as in environmental remediation, the solid species are easier to remove from the reaction medium, and therefore easier to recycle.

The effect of thermal treatment under H_2 flow on limonite surface and the effect of organic acids on the aqueous Fenton oxidation have been studied focusing on their acidity. But the role of organic acids as reagents able to enhance $^{\bullet}OH$ production has not been fully elucidated [10]. The literature proposes that H_2O_2 initiates a chain reaction that leads to the formation of $^{\bullet}OOH$ when in contact with Fe^{3+} sites available on the surface of goethite particles dispersed in aqueous solution [11].

These fixed Fe^{3+} sites are converted into fixed Fe^{2+} sites that react with H_2O_2 leading to the formation of $^{\bullet}OH$ radical (Eqs. (1)–(5)) and the recovering of the previous Fe^{3+} oxidation state

* Corresponding author. Fax: +55 35 3829 1271.
E-mail address: luizoliveira@ufla.br (L.C.A. Oliveira).
[1] Fax: +55 21 3865 6477.
[2] Fax: +55 35 3829 1271.

1381-1169/$ – see front matter © 2007 Elsevier B.V. All rights reserved.
doi:10.1016/j.molcata.2007.09.003

of these iron sites [11,12]:

$$H_2O_2 \xrightarrow{e^-} {}^{\bullet}OH + OH^- \quad (1)$$

$$H_2O_2 + HCOOH \xrightarrow{e^-} H_2O_2//HCOOH \quad (2)$$

$$H_2O_2//HCOOH \xrightarrow{e^-} {}^{\bullet}OH + H_2O + HCOO^- \quad (3)$$

$$H_2O_2 \ldots H^+ \xrightarrow{e^-} {}^{\bullet}OH + H_2O \quad (4)$$

$$H_2O_2//HCOOH \ldots H^+ \xrightarrow{e^-} {}^{\bullet}OH + H_2O + HCOOH \quad (5)$$

In the present work, the reactivity of the heterogeneous Fenton system HCOOC//H_2O_2 using thermal treated limonite was studied. Experiments were carried out to investigate the effect of formic acid contents and Fe^{2+} sites in iron oxide applied to the methylene blue degradation, using a Fenton-like heterogeneous system comprised of HCOOH and H_2O_2. The reactions were monitored by UV/vis and ESI-MS.

2. Materials and methods

2.1. Catalyst preparation and characterization

Limonite ore samples (45–46 wt% of Fe), from mines located in Goias State (Central Brazil), were ground and sieved below 100 mesh (Tyler series), dried for 1 h at 120 °C and then submitted to thermal treatment under H_2 flow (100 mL min^{-1}) at 350 °C for 10 and 60 min, aiming to form Fe^{2+} reduced sites from goethite phase (Fe^{3+}). Natural and reduced limonite samples were analyzed by FTIR using an Excalibur FTS3000 from Bio Rad, powder XRD (Ni filtered Co Kα radiation, λ = 0.17889 nm); room temperature Mössbauer spectroscopy (57Co/Rh source; isomer shifts are quoted relative to the α-Fe) and scanning electron microscopy (SEM) (Jeol-JKA 8900RL with Au sputtering coated samples fixed in a carbon tape). TPR experiments were performed in a CHEMBET 3000 equipment with 20 mg sample under 25 mL min^{-1} H_2 (5%)/N_2 with heating rate of 10 °C min^{-1}. N_2 adsorption/desorption isotherms were performed in an Autosorb 1, Quantachrome.

2.2. Oxidative reactions

Two types of reactions were carried out in the composite presence, according to the substrate: (i) the H_2O_2 decomposition to O_2 in water and (ii) the methylene blue dye oxidation (Fig. 1).

The former is typical hydrogen peroxide decomposition and was carried out in the flowing proportion, 2 mL of H_2O_2 solution (30%, v/v), 5 mL of water and 30 mg of the composite. The mixture was stirred with a magnetic rod stirrer and the reaction was monitored by measuring the O_2 formation in a volumetric glass system. The catalytic activity of the materials was tested for its effectiveness on the discoloring of methylene blue (10 mL of 50 mg L^{-1} stock solution) in an oxidant solution comprised of equimolar amounts of H_2O_2 and HCOOH (97 mmol). The oxidant solution was prepared 10 min before mixing with the dye and limonite.

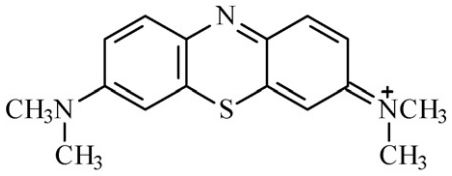

Fig. 1. Structure of the probe molecule (methylene blue dye).

2.3. ESI-MS study

In an attempt to identify the intermediates formed, the methylene blue dye decomposition was monitored using an electrospray ion source, an Agilent ion trap mass spectrometer (ESI-MS). The reaction samples were analyzed by introducing aliquots into the ESI source with a syringe pump at a flow rate of 5 μL min^{-1}. The spectrum obtained were an average of 50 scans of 0.2 s. Typical ESI-MS conditions were as follows: heated capillary temperature, 150 °C; dry gas (N_2) at a flow rate of 5 L min^{-1}; spray voltage 4 kV; capillary voltage 25 V; tube lens offset voltage, 25 V. For ESI-MS/MS, the parent ion of interest was first isolated by applying an appropriate waveform across the end cap electrodes of the ion trap to resonantly eject all trapped ions, except those ions with *m/z* ratio of interest. The isolated ions were then subjected to a supplementary ac signal, to resonantly excite them to cause collision-induced dissociation (CID) using helium as a reagent gas. The collision energy was set to a value in which ions were produced in measurable abundance.

The iron leaching during all reactions were evaluated by atomic absorption analysis, using a Varian AA 110 equipment. We found 0.065 and 0.078 mg L^{-1} of iron leaching from the samples of limonite 350 °C/10 min and 350 °C/60 min, respectively. We observed that this concentration of iron does not lead to a homogeneous Fenton reaction.

2.4. Computational methods

The calculations were carried out with the *Gaussian98* package [13]. All transition states, intermediates and precursors involved were calculated. Each conformer was fully optimized by DFT [14]. The energy profile at selected DFT geometries along the reaction pathway was computed at the B3LYP level of theory by using the 6-31+G(d,p) basis set. For all different calculation methods, the algorithms based on conjugate gradient and quasi-Newton–Raphson were used for the geometry optimization, until reaching a gradient of 10^{-9} atomic units. The final geometries were obtained with DFT by using the Becke's three-parameter hybrid functional with the LYP correlation functional [15] and density functional B3LYP using the basis set 6-311+G** [16]. This same computational procedure was also used elsewhere for similar systems, with good results [17,18]. Furthermore, after each optimization, the nature of the stationary point was established by calculating and diagonalizing the Hessian matrix (force constant matrix). The unique imaginary frequency associated with the transition vector (TV)

[19], *i.e.*, the eigenvector associated with the unique negative eigenvalue of the force constant matrix, was characterized. The solvent effect was evaluated with the polarized continuum model (PCM), initially proposed by Barone et al. [20], with the functional B3LYP and basis set 6-31+G(d,p). The solute cavity can then be specified as being any set of overlapping spheres. By representing the atoms as spheres, a more realistic cavity shape was produced for extended molecules, in contrast to other models of solvation [20].

3. Results and discussion

3.1. XRD and Mössbauer spectroscopy

The XRD patterns obtained (Fig. 2) suggested the presence of poorly crystalline goethite in the natural limonite sample with broad lines with lattice parameter values of 0.417, 0.269 and 0.245 nm. After thermal treatment the magnetite, Fe_3O_4, signals appeared in XRD with lattice parameters of 0.253, 0.297 and 0.147 nm.

Mössbauer characterizations of limonites are presented in Fig. 3a. In the case of natural limonite the iron oxide is presented in small particle size evidenced by a strong central duplet due to the super-paramagnetism phenomenal and a sextet with narrow lines and a hyperfine field (B_{hf}) of 37.8 T. The super-paramagnetic behaviour of goethite has been attributed both to a reduced magnetic coupling between the crystallites and to a relatively high concentration of vacancy defects [21]. The room temperature spectrum of the thermal treated limonite clearly shows tetrahedral (A) and octahedral (B) site formation characteristic of the magnetite phase with B_{hf} of 47 and 45 T, respectively (Table 1).

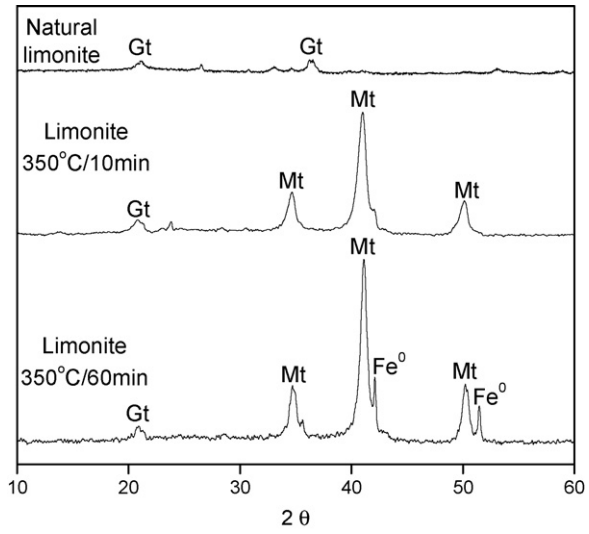

Fig. 2. XRD of natural and thermal treated limonites (Mt = magnetite and Gt = goethite).

Fig. 3b clearly shows the iron phase distribution obtained from the Mössbauer analyses. The results showed that the treatment for 10 min caused the reduction of goethite to magnetite producing a cubic structure with many cationic vacancies, according to XRD analysis. On the other hand, the treatment for 60 min converted the natural limonite into magnetite and Fe^0. These phase transformations are shown in Eqs. (6) and (7):

$$\alpha\text{-FeOOH} + H_2\,(350\,^{\circ}\text{C–}10\,\text{min}) \rightarrow Fe_3O_4\,(\text{magnetite}) \quad (6)$$

$$\alpha\text{-FeOOH} + H_2\,(350\,^{\circ}\text{C–}60\,\text{min}) \rightarrow Fe_3O_4\,(\text{magnetite}) + Fe^0 \quad (7)$$

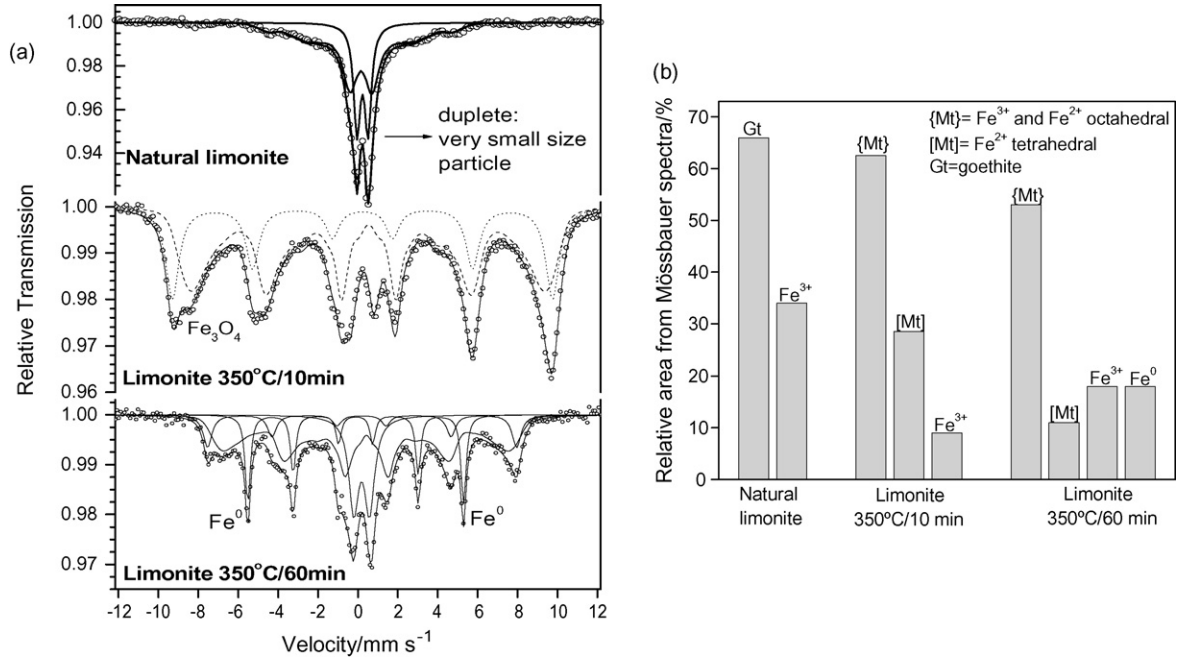

Fig. 3. Mössbauer spectrum limonite series (a) and phase distribution obtained from the Mössbauer data (b).

Table 1
Fitted room temperature Mössbauer parameters for limonites (δ = isomer shift relative to α-Fe, ε = quadruple shift, Δ = quadruple splitting, B_{hf} = hyperfine field, Γ = sub-spectrum middle height line width and RA = relative sub-spectral area)

Sample	Site ^{57}Fe	δ (mm s^{-1})	ε, Δ (mm s^{-1})	B_{hf} (T)	Γ (mm s^{-1})	RA (%)
Natural limonite	Limonite	0.329(3)	−0.25(2)	37.8(1)	0.31(2)	66(2)
	$^{VI}Fe^{3+}$	0.315(2)	0.60(1)		0.46(2)	34(2)
Limonite 350 °C/60 min	[Mt]	0.306(1)	0.03(2)	48.0(2)	0.52(2)	11(2)
	{Mt}	0.536(3)	−0.02(1)	45.8(3)	0.38(2)	53(2)
	$^{VI}Fe^{3+}$	0.301(2)	0.80(3)		0.60(2)	18(2)
	Fe^0	0	0	33.5(1)	0.31(2)	18(2)
Limonite 350 °C/10 min	{Mt}	0.534(4)	−0.019(2)	45.0(1)	0.38(2)	62.5(2)
	[Mt]	0.290(2)	−0.007(9)	47.8(2)	0.65(2)	28.5(2)
	Fe^{3+}	0.280(5)	1.01(1)		0.52(2)	9.0(2)

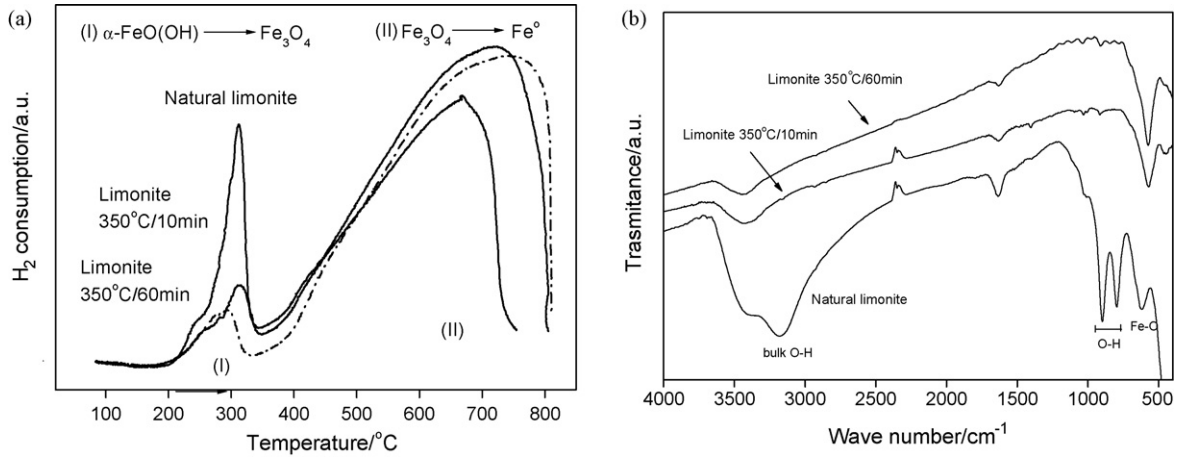

Fig. 4. TPR profiles (a) and FTIR (b) of catalysts before and after thermal treatment at 350 °C with H_2.

3.2. TPR and FTIR

The temperature programmed reduction (TPR) profile of the natural limonite presented a peak centred at 300 °C with a shoulder at ca. 210 °C and a broad peak from 400 to 800 °C. The materials were treated at 350 °C for 10 or 60 min because at this temperature the formation of an iron reduced phase occurs as suggested by process (I) in Fig. 4a. However, the reduction is not complete and a certain quantity of iron in Fe^{3+} form remains. These results agree with XRD and Mössbauer data.

Fig. 4b shows the infrared spectroscopy analyses. A typical signal for goethite phase is an intense band due to the bulk stretch, which is observed at 3140 cm^{-1}. Moreover, O–H bending bands at 792 and 901 cm^{-1}, which vibrate in and out of the plane, respectively, are important diagnostic bands for the goethite phase. It is important to observe that these two bands disappear after the thermal treatment. These results and the Fe–O vibration band at *ca.* 570 cm^{-1} suggest the magnetite phase formation.

3.3. H_2O_2 decomposition and dye oxidation

The catalytic activity of the limonite series was studied using two reactions: (i) the H_2O_2 decomposition to O_2 and (ii) the oxidation of methylene blue dye with H_2O_2 and formic acid in aqueous medium.

The H_2O_2 decompositions in the presence of different limonites are presented in Fig. 5. It is observed that the materials treated under H_2 flow (limonite 350 °C/10 min and limonite 350 °C/60 min) strongly favored the H_2O_2 decom-

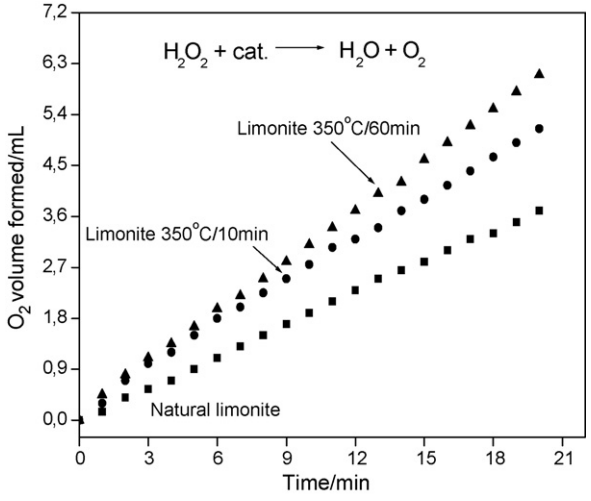

Fig. 5. Decomposition of H_2O_2 in the presence of limonites.

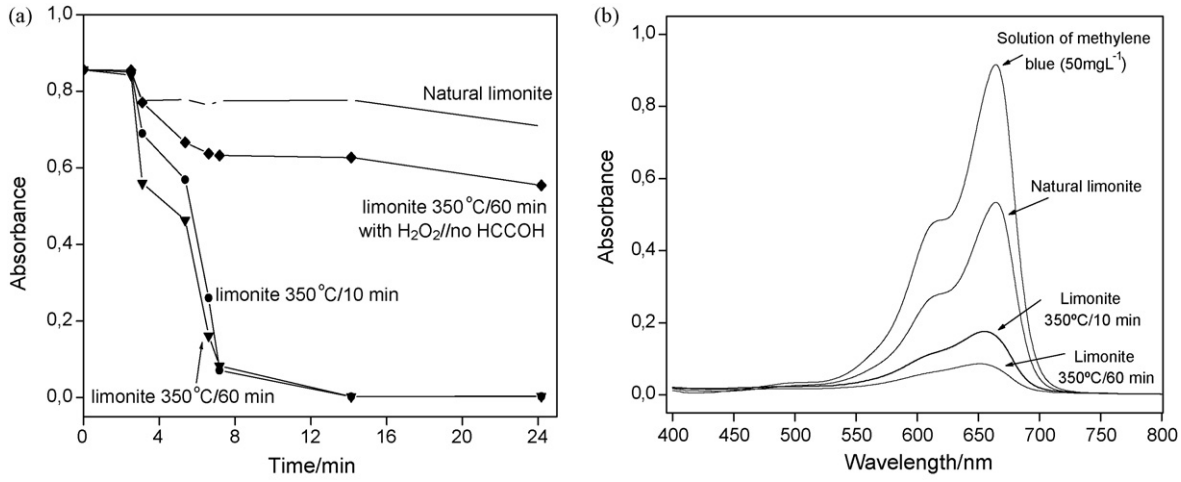

Fig. 6. Discoloration of methylene blue dye with H_2O_2//HCOOH in the presence limonites (a) and UV–vis spectrum after 7 min of reaction with limonites//H_2O_2//HCOOH (b).

position. These results show that the reduction of iron phase improves the activity in the H_2O_2 decomposition.

Fig. 6 shows the discoloration plots for methylene blue dye with H_2O_2//HCOOH in the presence of limonite. In a control experiment (only methylene blue dye and H_2O_2//HCOOH without limonites) there was no significant discoloration even after 30 min of reaction. Moreover, the limonite 350 °C/60 min presented a low activity for discoloration in absence of HCOOH (Fig. 6a). In our previous works [10] it was shown by theoretical DFT calculations that HCOOH interacts with H_2O_2 to form a stable H-bond linked system, which, upon acceptance of a single electron (for instance one electron released from Fe^{2+} in transition to Fe^{3+}), leads to a lower energy consumption path in the formation of Fenton reagent *OH than the H_2O_2/iron(II) system.

The literature shows that the conversion of Fe^{3+} sites to Fe^{2+} enhances Fenton oxidation of organic compounds [21]. Accordingly, the present work shows high methylene blue dye degradation over surfaces containing Fe^{2+} when compared to the surface containing Fe^{3+} of natural limonite. These results indicate that Fenton oxidation (of magnetite phase $^{\bullet}$OH attack) is taking place to some extent, which is remarkably improved by the presence of HCOOH, in agreement with the theoretical data [3]. The profile of methylene blue dye degradation in presence of H_2O_2//HCOOH in presence of natural limonite (containing only Fe^{3+}) showed a very different pattern from the thermally treated limonite one (containing Fe^{2+} sites). This suggests that Fenton oxidation is presumably taking place as well, probably due to Fe^{2+} sites formed from Fe^{3+}. Discoloration of organic dyes has attracted considerable attention in recent years. The most widely used catalytic process for dye removal is their oxidation with iron oxides in the presence of hydrogen peroxide. These materials have presented a good removal capacity, but the iron oxides employed are synthetic and must be modified (doped) to present some catalytic activity. For instance, the use of Cu-doped magnetite for discoloration Bromophenol Blue and Evans blue in aqueous medium after 100 min of reaction in the presence of H_2O_2 is described elsewhere [22]. Pure and doped goethites have been utilized in this reaction type, but the discoloration reaction is very slow; it takes place about 100 min to complete the reaction [23]. The thermal treatment with H_2, the presence of formic acid and the small particle size of the goethite in the natural limonite can be responsible for the high activity of the catalyst presented in this paper, as shown in Fig. 6.

Results (Fig. 6b) show that the 665 nm signal decreased as the reaction was occurring, according to the dye discoloration as shown in Fig. 6a. However, these results do not give any further evidence about the nature of intermediates formed during the oxidation process. Even though the complete discoloration of methylene blue was observed at less than 7 min of reaction

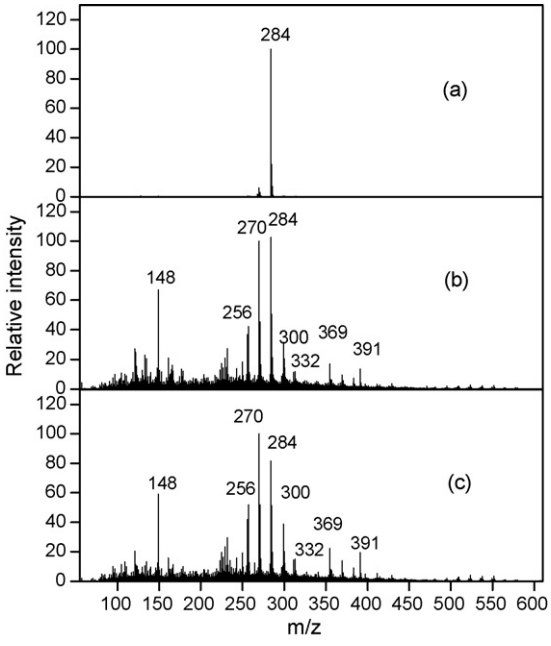

Fig. 7. ESI mass spectrum in the positive ion mode for monitoring the oxidation by the limonites//H_2O_2//HCOOH system of methylene blue dye in water. (a) Solution of methylene blue (50 mg L^{-1}); (b) limonite 350 °C/10 min; (c) limonite 350 °C/60 min.

(Fig. 6b) some intermediates might have been accumulated, and these chemical species may also be environmentally harmful [24].

Analyses by N_2 adsorption–desorption showed that the natural limonite samples, limonite 350 °C/10 min and limonite 350 °C/60 min present a surface area of 44, 30 and 19 $m^2\ g^{-1}$, respectively. These results suggest that the catalytic activity of the materials is not strongly affected by the BET surface area.

Results from the mass spectrometry analyses, applying the ESI for the screening of the oxidized species formed during the decomposition reaction of methylene blue dye with the limonites and H_2O_2//HCOOH system, are shown in Fig. 7. The ESI-MS spectrum obtained for the dye solution shows only a strong signal at $m/z = 284$, which is related to the methylene blue ion (Fig. 7a). After 7 min of reaction with the reduced limonite and hydrogen peroxide with HCOOH, some new m/z signals appear, for example, at 300 and 332 (Fig. 7b and c) indicating that the hydroxylation is occurring in the process. At this reaction time, other m/z signals appear ($m/z = 148$), likely related to methylene blue oxidation intermediates, also suggesting that the structural ring was somehow fragmented.

3.4. Theoretical calculations

In order to shed some more light on the model of the overall reaction mechanism, calculations of the Gibbs free energy for the stability of the intermediates were performed, by the algorithm implemented in the Gaussian98 package [13]. All discussions concerning the energy differences and the energy barriers refer to the enthalpy term corrected for the zero point energy at 298.15 K. The resulting energy values are presented in Table 2 and Fig. 8. From this calculation, a good agreement between the modeled and experimental geometry was found for the methylene blue molecule [20]. According to data listed in Table 2, it can be observed that the hydroxyl group on C2 position is about +3.30 and +6.65 kcal mol^{-1} more stable than the alternative C3 and C5, respectively. These results put in evidence that the preferential reaction site for •OH in this Fenton process is the position 2 (C2) of the methylene blue structure, resulting in an intense fragment corresponding to $m/z = 300$. From these theoretical results, compound **II** is supposed to be stable and can be experimentally detected, although no further attempt was made in this work to address this analysis. Moreover, the reaction path may still involve other hydroxylation. From these results, the third hydroxylation would more likely occur at 5′ position. This is crucial step, as it would simultaneously lead to the formation of hydroquinone or hydroquinone-like intermediates generated by the •OH attack. That is an unstable key-intermediate that points out the quick and high probability of rupture of both chemical bonds C1–C2 and C5–C6. This could justify the formation of **IV** ($m/z = 148$). Further and still more accurate theoretical calculations in order to verify this hypothesis are now in progress.

Table 2
Gibbs free energy of **II** and **III** intermediates using B3LYP/6-31+G(d,p)

Intermediate	Hydroxyl position	ΔG (kcal mol^{-1})
II	2	0.00
	3	+3.30
	5	+6.04

3.5. Catalyst deactivation

The limonites reduced for 10 and 60 min, limonite 350 °C/10 min and limonite 350 °C/60 min, respectively, were tested for methylene blue dye discoloration in reaction cycles (Fig. 9). The limonite 350 °C/10 min and 350 °C/60 min after three reaction cycles presented a loss of catalytic activity (Fig. 9a), suggesting that the Fe^{2+} oxidation occurs on the sur-

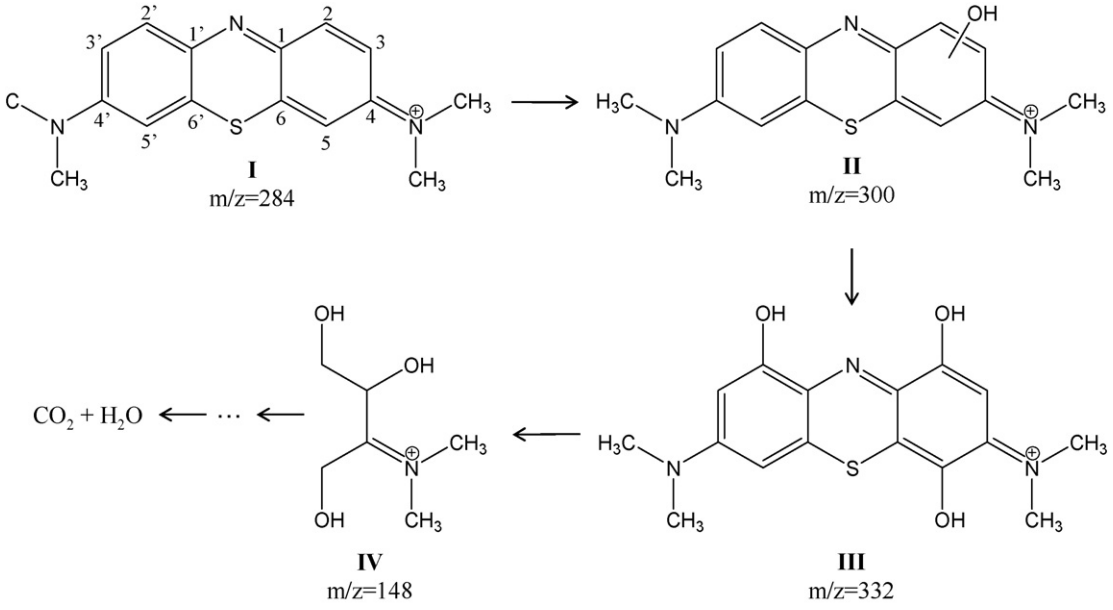

Fig. 8. Scheme with proposed intermediates for the oxidation of methylene blue dye ($m/z = 284$) by the limonites.

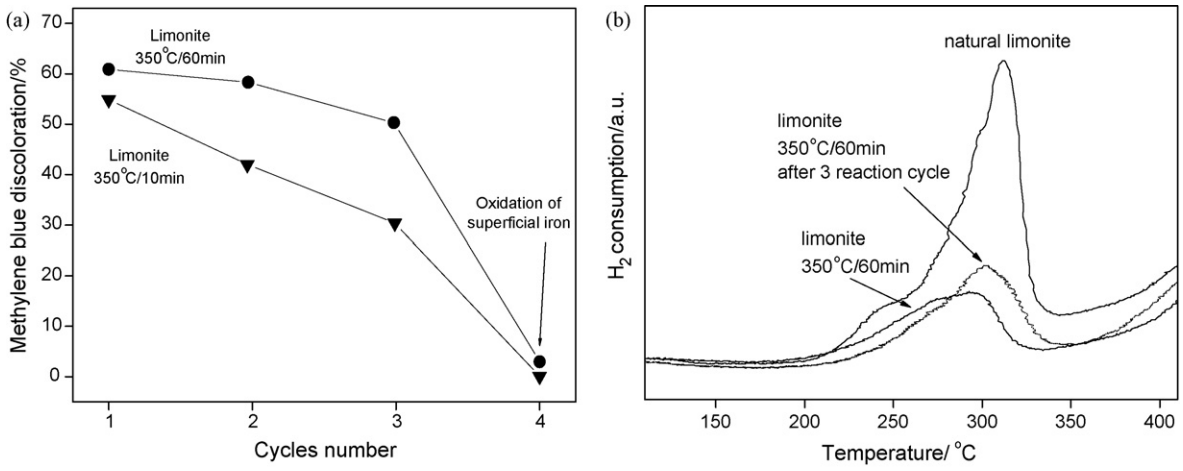

Fig. 9. Reaction cycle of methylene blue dye discoloration (a) and TPR profiles after oxidation reaction of the thermally treated catalyst for 60 min (b).

face of the limonite. Moreover, the activity loss is lower for limonite 350 °C/60 min, probably due to the Fe^0 presence that can regenerate the Fe^{2+} sites by donating electrons, as described in the literature [25].

The limonite 350 °C/60 min catalyst, after three reaction cycles, was characterized by TPR (Fig. 9b). It is possible to note an increase of the un-reduced phase *ca.* 300 °C in the catalyst. The calculation of the area under the curves shows that approximately 34% of oxidized phase was formed on the surface of the catalysts, suggesting that the deactivation (Fig. 9a) might be due to Fe^{2+} oxidation on the surface of thermal treated limonites.

4. Conclusion

We showed that the chemical properties of natural limonite can strongly be modified when treated with H_2 to form reduced iron oxide phase. The resulting materials showed a remarkable effect on the discoloration of an organic dye in aqueous medium. ESI-MS studies of the methylene blue oxidation showed successive hydroxylations as intermediate species.

Fenton-type degradation of an organic contaminant by H_2O_2 over an iron oxide surface is remarkably enhanced by the presence of HCOOH. The degradation capacity is also enhanced by the presence of Fe^{2+} sites on the iron oxide surface after the thermal treatment under H_2 atmosphere, indicating that Fenton reagent $^{\bullet}OH$ attack is taking place.

Acknowledgments

The authors are grateful to CENPES-Petrobras for financial support, Prof. José Domingos Fabris (UFMG-Brazil) for Mössbauer analyses and Prof. Teodorico Ramalho for the computational calculations.

References

[1] W.F. de Souza, US Patent 6,544,409 (2003).
[2] W.F. de Souza, US Patent 0108252 (2004).
[3] W.F. de Souza, L. Ernst, BR PI Patent 0405847 (2005).
[4] M. Lu, J. Chen, H. Huang, Chemosphere 46 (2002) 131.
[5] S. Chou, C. Huang, Chemosphere 38 (1999) 2719.
[6] B.W. Tyre, R.J. Watts, G.C. Miller, J. Environ. Qual. 20 (1991) 832.
[7] W.P. Kwan, B.M. Voelker, Environ. Sci. Technol. 36 (2002) 1467.
[8] I.W.C.E. Arends, R. Sheldon, Appl. Catal. A: Gen. 212 (2001) 175.
[9] L. Menini, M.J. da Silva, M.F.F. Lelis, J.D. Fabris, R.M. Lago, E.V. Gusevskaya, Appl. Catal. A: Gen. 269 (2004) 117.
[10] W. Ferraz, L.C.A. Oliveira, R. Dallago, L. da Conceição, Catal. Commun. 8 (2007) 131.
[11] B. Ensing, Doctor Thesis, Vrije University, Amsterdam, Holland, 2003.
[12] R.L. Valentine, H.C.A. Wang, J. Environ. Eng.: ASCE 124 (1998) 31.
[13] M.J. Frisch, G.W. Trucks, H.B. Schlegel, G.E. Scuseria, M.A. Robb, J.R. Cheeseman, J.A. Montgomery Jr., T. Vreven, K.N. Kudin, J.C. Burant, J.M. Millam, S.S. Iyengar, J. Tomasi, V. Barone, B. Mennucci, M. Cossi, G. Scalmani, N. Rega, G.A. Petersson, H. Nakatsuji, M. Hada, M. Ehara, K. Toyota, R. Fukuda, J. Hasegawa, M. Ishida, T. Nakajima, Y. Honda, O. Kitao, H. Nakai, M. Klene, X. Li, J.E. Knox, H.P. Hratchian, J.B. Cross, V. Bakken, C. Adamo, J. Jaramillo, R. Gomperts, R.E. Stratmann, O. Yazyev, A.J. Austin, R. Cammi, C. Pomelli, J.W. Ochterski, P.Y. Ayala, K. Morokuma, G.A. Voth, P. Salvador, J.J. Dannenberg, V.G. Zakrzewski, S. Dapprich, A.D. Daniels, M.C. Strain, O. Farkas, D.K. Malick, A.D. Rabuck, K. Raghavachari, J.B. Foresman, J.V. Ortiz, Q. Cui, A.G. Baboul, S. Clifford, J. Cioslowski, B.B. Stefanov, G. Liu, A. Liashenko, P. Piskorz, I. Komaromi, R.L. Martin, D.J. Fox, T. Keith, M.A. Al-Laham, C.Y. Peng, A. Nanayakkara, M. Challacombe, P.M.W. Gill, B. Johnson, W. Chen, M.W. Wong, C. Gonzalez, J.A. Pople, Gaussian 98, Revision A.9, Gaussian, Inc., Wallingford, CT, 1998.
[14] H.G. Li, G.K. Kim, C.K. Kim, S. Rhee, I. Lee, J. Am. Chem. Soc. 123 (2001) 2326.
[15] A.D. Becke, J. Chem. Phys. 98 (1993) 5648.
[16] S. El-Taher, R.H. Hilal, Int. J. Quantum Chem. 20 (2001) 242.
[17] T.C. Ramalho, M. Buhl, Magn. Reson. Chem. 43 (2005) 139.
[18] E.F.F. da Cunha, T.C. Ramalho, R.B. de Alencastro, C.A. Taft, Lett. Drug Des. Discov. 3 (2006) 625.
[19] J.W. McIver Jr., Chem. Res. 7 (1994) 72.
[20] V. Barone, M. Cossi, J.J. Tomasi, Comput. Chem. 19 (1998) 404.
[21] H.H. Kilen, A.B. Thomsen, Water Res. 32 (1998) 3353.
[22] P. Baldrian, V. Merhautova, J. Gabriel, F. Nerud, P. Stopka, M. Hruby, M.J. Benes, Appl. Catal. B: Environ. 66 (2006) 258.
[23] L.C.A. Oliveira, M. Gonçalves, D.Q.L. Oliveira, A.L. Guarieiro, M.C. Pereira, Quím. Nova 30 (2007) 925.
[24] L.C.A. Oliveira, M. Gonçalves, M.C. Guerreiro, T.C. Ramalho, J.D. Fabris, M.C. Pereira, K. Sapag, Appl. Catal. A: Gen. 316 (2007) 117.
[25] F.C.C. Moura, G.C. Oliveira, M.H. Araújo, J.D. Ardisson, W.A.A. Macedo, R.M. Lago, Appl. Catal. A: Gen. 307 (2006) 195.